mekatronika – Journal of Intelligent Manufacturing & Mechatronics
VOL. 01, ISSUE 02, 45 – 65
DOI: https://doi.org/10.15282/mekatronika.v1i2.4986

ORIGINAL ARTICLE

Fitness-evaluated Adaptive Switching Simulated Kalman Filter Algorithm with Randomness

Nor Azlina Ab. Aziz[1], Tasiransurini Ab Rahman[2] and Nor Hidayati Abdul Aziz[1]

[1]Faculty of Engineering and Technology, Multimedia University, Melaka, Malaysia.
[2]Faculty of Electrical and Electronic Engineering, Universiti Tun Hussein Onn Malaysia, Johor, Malaysia.

ABSTRACT – The original Simulated Kalman Filter (SKF) is an optimizer that employs synchronous update mechanism. The agents in SKF update their solutions after all fitness calculations, prediction process, and measurement process are completed. An alternative to synchronous update is asynchronous update. In asynchronous update, only one agent does fitness calculation, prediction, measurement, and estimation processes at one time. A recent study shows that the asynchronous SKF outperforms synchronous SKF. In this study, synchronous and asynchronous mechanisms are combined in SKF. At first, the SKF starts with either synchronous or asynchronous update. By evaluating the fitness, if no improved solution is found, the SKF changes its update mechanism. The decision to switch from synchronous to asynchronous or vice versa is made randomly. Using the CEC2014 benchmark test suite, experimental results indicate that the proposed adaptive switching SKF randomness outperforms the original SKF algorithm.

ARTICLE HISTORY
Received: 19 January 2019
Accepted: 9 March 2019

KEYWORDS
Optimization
SKF
Randomness

Introduction

A metaheuristic is an iterative generation process which guides a subordinate heuristic by combining intelligently different concepts for exploring and exploiting the search space so that a near-optimal solution can be obtained. In 2015, a new metaheuristic algorithm called simulated Kalman filter (SKF), has been introduced for numerical optimization problems [1-3]. It was introduced as population-based metaheuristics, where the search for optimal solution is conducted by a group of agents. The agents of SKF work like Kalman filters [4], where they go through prediction, measurement, and estimation process in every iteration. The measurement in SKF is a simulated measurement which is obtained using mathematical equation.

As a population-based metaheuristic algorithm, the SKF's agents conduct the search for optimal solution through information sharing. The evaluation of the candidate solutions found by SKF agents and the Kalman filter's procedure of predict, measure and estimate are done iteratively. How the agents move from evaluation to the Kalman procedure, either as a group or individually is determined by the iteration strategy. The group-oriented iteration strategy is known as synchronous update while the individual-oriented iteration strategy is known as asynchronous update. So far, most studies on SKF have been carried out based on synchronous update implementation, where every agent of the population need to complete the evaluation phase before the Kalman phase can begin.

Many studies on SKF can be found in literature. For example, the SKF has been studied fundamentally [5-6]. The SKF also has been extended for binary optimization problems [7] and combinatorial optimization problems [8-10]. Hybridization of SKF with particle swarm optimization (PSO), gravitational search algorithm (GSA), and opposition-based learning [11-16] have also been proposed for better performance. Other variants called parameter-less SKF and randomized SKF algorithms were proposed in [17-18]. The SKF has also been applied for real world problems like the adaptive beamforming in wireless cellular communication [19-22], airport gate allocation problem [23-24], feature selection of EEG signal [25-26], system identification [27-28], image processing [29-30], assembly sequence planning [31], controller tuning [32], and PCB drill path optimization [33-34].

*CORRESPONDING AUTHOR | Nor Azlina Ab. Aziz | ✉ azlina.aziz@mmu.edu.my

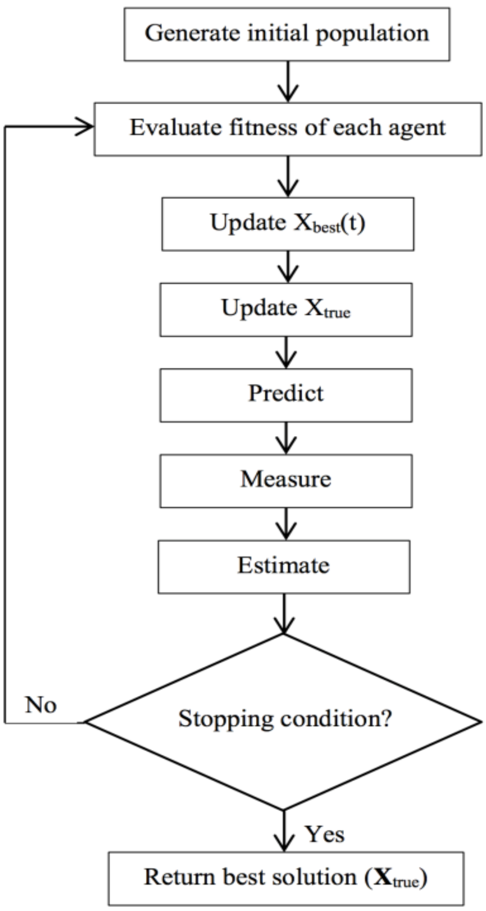

Figure 1. The flowchart of the SKF.

Recently, asynchronous sequence update in SKF has been studied [35]. In this work, a new variant of SKF is proposed. The proposed algorithm is called adaptive switching SKF with randomness (ASSKFR) which applies switching between synchronous and asynchronous updates based on a random process. There are two variants of ASSKFR algorithms. The first is ASSKFR$_a^{fit}$ that begins with asynchronous update. On the other hand, the ASSKFR$_s^{fit}$ begins with synchronous update. The performance of both ASSKFR variants are compared with the original SKF using CEC2014 benchmark function, where more accurate (less error) solutions can be obtained.

The Simulated Kalman Filter

The SKF algorithm follows the algorithm shown in Figure 1. One iteration consists of fitness evaluation, update the best solution, predict, measure, and estimate.

Using n agents, a set of solution can be denoted as $X(t) = \{X_1(t), X_2(t), \ldots, X_n(t)\}$, where t is the iteration number. The SKF starts with random initialization of solutions. In each iteration, the fitness of the agents' are evaluated. Then, the agent with the best fitness value is identified as the best solution of the current population, $X_{best}(t)$. Next, the best $X_{best}(t)$ from the first iteration is selected as X_{true}.

During the prediction phase, the current predicted state, $X_i(t|t+1)$, is assumed to be the estimated value:

$$X_i(t|t+1) = X_i(t) \tag{1}$$

The error covariant is also updated as follows:

$$P(t|t) = P(t) + Q \tag{2}$$

where $P(t)$ and $P(t|t+1)$ denote the current error covariant estimate and current transition error covariant estimate, respectively. Note that the error covariant estimate is influenced by the process noise, Q.

In SKF, measurements are simulated using an agent's prediction and X_{true}. The dimensional wise calculation of measured value for each dimension of agent ith is calculated as follows:

$$Z_i(t) = X_i(t|t) + \sin(2\pi r_i(t)) \times |X_i(t|t) - X_{true}| \tag{3}$$

where $r_i(t)$ is a random value within the range of [0,1]. The estimation phase follows the measurement phase and the estimated next value is updated using (4):

$$X_i(t+1) = X_i(t|t+1) + K(t) \times (Z_i(t) - X_i(t|t+1)) \tag{4}$$

where $K(t)$ is the Kalman gain, which is calculated as follows:

$$K(t) = P(t|t+1)/(P(t|t+1)+R) \tag{5}$$

where R is the measurement noise. Then, the current error covariant estimate is updated in estimation phase using (6):

$$P(t+1) = (1-K(t)) \times P(t|t+1) \tag{6}$$

These steps continue until at the end of the iteration or at the end of the fitness evaluation.

Note that this original SKF algorithm is also known as synchronous SKF. Another version of SKF is called asynchronous SKF (ASKF) [35]. Like the original SKF, ASKF starts with random initialization of the population according to the problem's search space. However, the steps within the iteration are individually executed for ASKF. Therefore, in an iteration of ASKF, as soon as an agent is evaluated, its fitness is compared with X_{true}. If the agent has found a better solution, then the X_{true} is immediately updated according to the estimated value of the agent. Thus, in ASKF, $X_{best}(t)$ is not needed.

mekatronika – Journal of Intelligent Manufacturing & Mechatronics
VOL. 01, ISSUE 02, 45 – 65
DOI: https://doi.org/10.15282/mekatronika.v1i2.4241

```
Initialization of agents
Do{
        For every agents
                Evaluate fitness
        End for
        Identify X_best(t)
        Update X_true
        For every agent
                Predict
                Measure
                Estimate
        End for
}While not maximum iteration
```

Figure 2. The synchronous SKF pseudocode.

```
Initialization of agents
Do{
        For every agents
                Evaluate fitness
                Update X_true
                Predict
                Measure
                Estimate
        End for
}While not maximum iteration
```

Figure 3. The asynchronous SKF pseudocode.

After the X_{true} comparison, the agent's state is immediately predicted. This is followed by the agent's measurement and state estimation. The prediction, measurement and estimation are carried using the same set of equations like the original SKF. When an agent completed its Kalman filter's procedures, next agent is selected to go through the same steps.

The difference between the synchronous SKF and asynchronous SKF is shown the pseudocodes in Figure 2 and Figure 3, respectively. Recent study shows that for numerical optimization problems, the asynchronous SKF is better than the synchronous SKF [35].

The Adaptive Switching SKF with Randomness

Random switching iteration strategy randomly alternates the iteration strategy SKF between the synchronous update and asynchronous update throughout the search. The proposed general flowchart of the fitness-evaluated adaptive switching SKF with randomness (ASSKFR) is shown in Figure 4. There are several important variables in this flowchart.

At first, the population switches its iteration strategy after Δ number of fitness evaluation. The value of Δ is randomly chosen every time a switching occurs. The range of Δ is drawn from uniform random distribution between zero to the maximum number of fitness evaluation (*FES*). No information of the population's condition is used in selecting the value of Δ.

The population switches between the two iteration strategies based on the switching counter, δ. Let fit be the best-so-far fitness. If *fit* is static, *fit*(t)/ *fit*(t-1) = 1, before next iteration begins, its switching counter, δ, is incremented and if $\delta \geq \Delta$ then the population switches its iteration strategy. If the iteration strategy switches, then δ is reset to zero.

Thus, the proposed ASSKFR_a^{fit} is a variant of adaptive switching SKF algorithm that adopts adaptive switching iteration strategy with randomness that uses fitness (*fit*) as its switching indicator and asynchronous update as the initial strategy, while ASSKFR_s^{fit} starts with synchronous update. Maximum number of fitness evaluation, FES, is used as the stopping condition. If the maximum number of fitness evaluation has been executed, the algorithm stops.

Experiment, Result, and Discussion

The performance of the proposed synchronous-asynchronous SKF with random switching is compared with the asynchronous SKF using CEC2014 Benchmark Test Suite [5] for single objective optimization. All the test problems are function minimization and the test suite comprise of 30 functions consisting mixture of three unimodal test

***CORRESPONDING AUTHOR** | Nor Azlina Ab. Aziz | ✉ azlina.aziz@mmu.edu.my

mekatronika – Journal of Intelligent Manufacturing & Mechatronics
VOL. 01, ISSUE 02, 45 – 65
DOI: https://doi.org/10.15282/mekatronika.v1i2.4241

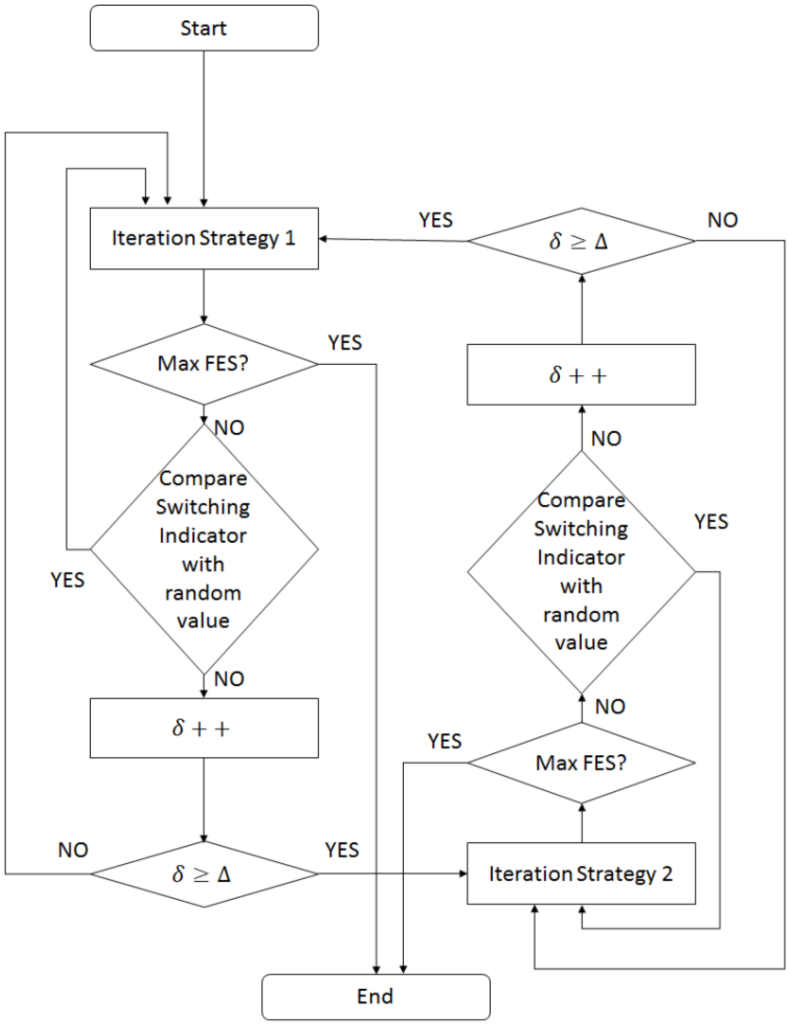

Figure 4. General flowchart of the fitness-evaluated adaptive switching SKF with randomness.

suite (f1-f3), 13 simple multimodal test suites (f4-f16), six hybrid test suites (f17-f22), and eight composition test suites (f23-30) as shown in Table 1. The ideal fitness values are included as well.

The comparison is conducted using population of 100 agents, dimension size of 30, and maximum iteration of 3000. Each of the experiment is run 30 times. Note that the $P(0)$, Q, and R values of SKF are 100, 0.5, and 0.5, respectively. Since the ideal fitness of each function is known, it is possible to calculate the error, which is the difference between the fitness value obtained and the ideal fitness. After 30 trials, the averaged error values are calculated.

Figure 5 and Figure 6 show the average fitness values from the ASSKFR_a^{fit} experiment. The values highlighted with boldface are the smallest average error value for the respective functions. The smallest values are distributed among ASSKFR_a^{fit} tested.

Wilcoxon signed rank test [37] was conducted and the statistical values are shown in Table 2. The statistic values show that ASSKFR_a^{fit} with all value of Δ is significantly better than SSKF. The value of Δ that allows a greater number of switching gave better significance level. ASSKFR_a^{fit} with Δ= {80%. 85%, 90%, 95%} had 10% significance level while others' significance level is 1%. Comparison of ASSKFR_a^{fit} with ASKF found that Δ= {50%, 55%, 65%, 70%, 80%, 85%, 90%} performed on par with ASKF. ASSKFR_a^{fit} with other values of Δ has better performance than ASKF with significance level of at least 10%.

*CORRESPONDING AUTHOR | Nor Azlina Ab. Aziz | ✉ azlina.aziz@mmu.edu.my

mekatronika – Journal of Intelligent Manufacturing & Mechatronics
VOL. 01, ISSUE 02, 45 – 65
DOI: https://doi.org/10.15282/mekatronika.v1i2.4241

Table 1. The CEC2014 test suite.

Function	Type of function	Ideal fitness
f1	Rotated High Conditioned Elliptic	100
f2	Rotated Bent Cigar	200
f3	Rotated Discus	300
f4	Shifted and Rotated Rosenbrock’s	400
f5	Shifted and Rotated Ackley’s	500
f6	Shifted and Rotated Weierstrass	600
f7	Shifted and Rotated Griewank’s	700
f8	Shifted Rastrigin’s	800
f9	Shifted and Rotated Rastrigin’s	900
f10	Shifted Schwefel’s	1000
f11	Shifted and Rotated Schwefel’s	1100
f12	Shifted and Rotated Katsura	1200
f13	Shifted and Rotated HappyCat	1300
f14	Shifted and Rotated HGBat	1400
f15	Shifted and Rotated Expanded Griewank’s plus Rosenbrock’s	1500
f16	Shifted and Rotated Expanded Scaffer’s	1600
f17	Hybrid function 1 (N=3)	1700
f18	Hybrid function 2 (N=3)	1800
f19	Hybrid function 3 (N=4)	1900
f20	Hybrid function 4 (N=4)	2000
f21	Hybrid function 5 (N=5)	2100
f22	Hybrid function 6 (N=6)	2200
f23	Composition function 1 (N=5)	2300
f24	Composition function 2 (N=3)	2400
f25	Composition function 3 (N=3)	2500
f26	Composition function 4 (N=5)	2600
f27	Composition function 5 (N=5)	2700
f28	Composition function 6 (N=5)	2800
f29	Composition function 7 (N=3)	2900
f30	Composition function 8 (N=3)	3000

Function ID	S-SKF	A-SKF	5%	10%	15%	20%	25%	30%	35%	40%	45%	50%
f1	4.860E+05	1.100E+07	2.630E+05	2.960E+05	3.790E+05	2.920E+05	2.750E+05	4.460E+05	4.650E+05	4.370E+05	3.160E+05	**2.040E+05**
f2	2.450E+08	1.290E+06	7.990E+05	**2.764E+04**	3.050E+06	3.540E+05	1.340E+06	1.700E+06	3.410E+05	3.130E+06	7.150E+06	3.830E+07
f3	1.841E+04	9.901E+03	**5.589E+03**	7.212E+03	6.778E+03	9.718E+03	7.842E+03	8.553E+03	9.284E+03	7.695E+03	9.962E+03	9.413E+03
f4	3.646E+01	1.177E+02	1.376E+01	**7.984E+00**	1.811E+01	2.175E+01	1.526E+01	2.922E+01	2.745E+01	3.276E+01	2.250E+01	2.249E+01
f5	2.002E+01	2.001E+01	**2.000E+01**	2.000E+01	**2.000E+01**	**2.000E+01**	2.000E+01	2.000E+01	2.000E+01	2.000E+01	2.000E+01	2.000E+01
f6	2.195E+01	1.817E+01	1.588E+01	**1.462E+01**	1.499E+01	1.708E+01	1.546E+01	1.600E+01	1.720E+01	1.816E+01	1.531E+01	1.618E+01
f7	1.635E-01	8.444E-02	7.778E-02	8.983E-02	7.148E-02	**5.172E-02**	6.199E-02	5.773E-02	6.738E-02	7.675E-02	1.704E-01	1.336E-01
f8	5.878E+00	5.473E+00	**6.966E-01**	1.858E+00	1.980E+00	3.282E+00	3.647E+00	3.825E+00	4.037E+00	4.090E+00	4.813E+00	7.340E+00
f9	9.087E+01	7.526E+01	7.582E+01	7.499E+01	6.866E+01	7.469E+01	7.607E+01	**6.656E+01**	7.076E+01	8.060E+01	7.060E+01	7.061E+01
f10	2.263E+02	1.620E+02	**3.781E+01**	8.057E+01	1.235E+02	1.232E+02	1.276E+02	1.478E+02	1.329E+02	1.436E+02	1.514E+02	1.986E+02
f11	2.640E+03	2.585E+03	2.580E+03	2.486E+03	2.406E+03	**2.393E+03**	2.447E+03	2.480E+03	2.509E+03	2.539E+03	2.483E+03	2.563E+03
f12	3.592E-01	2.099E-01	1.997E-01	**1.825E-01**	2.197E-01	2.184E-01	1.860E-01	1.991E-01	2.184E-01	2.055E-01	2.361E-01	2.153E-01
f13	4.443E-01	3.567E-01	3.458E-01	3.612E-01	3.629E-01	3.442E-01	3.507E-01	3.480E-01	3.545E-01	3.457E-01	3.353E-01	3.550E-01
f14	2.593E-01	2.273E-01	2.336E-01	2.319E-01	2.224E-01	2.239E-01	2.358E-01	2.299E-01	2.287E-01	2.225E-01	2.220E-01	2.321E-01
f15	2.192E+01	1.640E+01	1.757E+01	1.669E+01	1.436E+01	1.556E+01	1.304E+01	1.400E+01	1.326E+01	1.327E+01	1.674E+01	1.501E+01
f16	1.060E+01	1.067E+01	**1.021E+01**	1.028E+01	1.045E+01	1.046E+01	1.051E+01	1.040E+01	1.047E+01	1.034E+01	1.056E+01	1.058E+01
f17	1.050E+05	1.170E+06	1.070E+05	**1.030E+05**	1.410E+05	1.250E+05	1.150E+05	1.590E+05	1.540E+05	1.370E+05	1.240E+05	1.620E+05
f18	1.150E+07	8.560E+06	1.510E+03	1.903E+03	**1.265E+03**	1.806E+03	6.698E+03	1.884E+03	4.921E+03	1.377E+03	5.028E+04	2.370E+06
f19	2.050E+01	1.985E+01	1.234E+01	1.212E+01	**8.928E+00**	1.453E+01	1.237E+01	1.092E+01	2.280E+01	2.024E+01	1.525E+01	1.305E+01
f20	2.984E+04	2.415E+04	**6.607E+03**	7.957E+03	1.206E+04	1.332E+04	1.761E+04	1.434E+04	1.784E+04	1.645E+04	1.821E+04	2.226E+04
f21	2.610E+05	5.550E+05	1.570E+05	1.640E+05	1.740E+05	1.900E+05	**1.350E+05**	2.130E+05	2.420E+05	1.800E+05	2.080E+05	2.040E+05
f22	6.217E+02	4.973E+02	4.800E+02	5.429E+02	5.071E+02	5.256E+02	5.523E+02	5.581E+02	5.276E+02	5.074E+02	5.190E+02	5.292E+02
f23	3.181E+02	3.161E+02	**3.159E+02**	3.164E+02	3.160E+02	3.161E+02	3.162E+02	3.160E+02	3.161E+02	3.163E+02	3.163E+02	3.166E+02
f24	2.310E+02	2.292E+02	**2.269E+02**	2.278E+02	2.273E+02	2.280E+02	2.282E+02	2.277E+02	2.280E+02	2.288E+02	2.275E+02	2.295E+02
f25	2.151E+02	2.143E+02	2.141E+02	2.152E+02	**2.138E+02**	2.143E+02	2.145E+02	2.145E+02	2.143E+02	2.141E+02	2.149E+02	2.138E+02
f26	1.204E+02	1.204E+02	**1.004E+02**	1.037E+02	1.070E+02	1.037E+02	1.103E+02	1.038E+02	1.137E+02	1.137E+02	1.204E+02	1.303E+02
f27	5.985E+02	5.476E+02	5.682E+02	6.004E+02	6.059E+02	5.855E+02	6.140E+02	**4.954E+02**	5.201E+02	6.145E+02	6.127E+02	6.109E+02
f28	1.574E+03	1.610E+03	1.698E+03	1.700E+03	1.580E+03	1.630E+03	1.516E+03	1.545E+03	1.713E+03	1.595E+03	1.543E+03	1.635E+03
f29	2.477E+03	1.189E+03	1.006E+03	9.544E+02	1.009E+03	1.035E+03	1.002E+03	**9.412E+02**	1.123E+03	1.013E+03	1.036E+03	1.003E+03
f30	5.438E+03	3.848E+03	**2.490E+03**	2.820E+03	2.994E+03	3.009E+03	2.926E+03	3.050E+03	3.278E+03	3.122E+03	3.197E+03	3.165E+03

Figure 5. Result of the ASSKFR$_a^{fit}$ experiment (Δ= {5%, 10%, 15%, 20%, 25%, 30%, 35%, 40%, 45%, 50%}).

*CORRESPONDING AUTHOR | Nor Azlina Ab. Aziz | ✉ azlina.aziz@mmu.edu.my

Function ID	S-SKF	A-SKF	55%	60%	65%	70%	75%	80%	85%	90%	95%
f1	4.860E+05	1.100E+07	2.840E+05	4.680E+05	4.570E+05	3.720E+05	3.270E+05	4.480E+05	9.480E+05	1.130E+06	3.440E+06
f2	2.450E+08	1.290E+06	7.920E+06	5.110E+06	2.650E+07	2.140E+07	2.380E+06	9.050E+06	1.170E+07	1.800E+07	9.270E+06
f3	1.841E+04	9.901E+03	1.152E+04	1.143E+04	1.057E+04	9.612E+03	1.233E+04	9.341E+03	9.408E+03	1.194E+04	9.489E+03
f4	3.646E+01	1.177E+02	3.094E+01	1.708E+01	2.040E+01	2.909E+01	2.680E+01	5.726E+01	5.254E+01	4.898E+01	6.502E+01
f5	2.002E+01	2.001E+01	2.001E+01	2.001E+01	2.001E+01	2.001E+01	2.001E+01	2.001E+01	2.001E+01	2.001E+01	2.001E+01
f6	2.195E+01	1.817E+01	2.416E+01	1.704E+01	1.699E+01	1.851E+01	1.724E+01	1.761E+01	1.627E+01	1.678E+01	1.772E+01
f7	1.635E-01	8.444E-02	1.167E-01	1.108E-01	7.989E-02	7.960E-02	8.257E-02	9.816E-02	1.223E-01	7.812E-02	8.342E-02
f8	5.878E+00	5.473E+00	6.689E+00	5.921E+00	6.635E+00	7.318E+00	5.754E+00	4.682E+00	5.738E+00	5.395E+00	4.853E+00
f9	9.087E+01	7.526E+01	7.173E+01	7.466E+01	7.642E+01	7.807E+01	7.496E+01	7.573E+01	7.708E+01	7.714E+01	6.785E+01
f10	2.263E+02	1.620E+02	2.279E+02	2.615E+02	1.966E+02	2.661E+02	1.670E+02	2.406E+02	2.033E+02	1.945E+02	1.918E+02
f11	2.640E+03	2.585E+03	2.434E+03	2.497E+03	2.710E+03	2.512E+03	2.717E+03	2.659E+03	2.664E+03	2.610E+03	2.734E+03
f12	3.592E-01	2.099E-01	2.387E-01	2.085E-01	2.413E-01	2.069E-01	2.231E-01	2.128E-01	2.324E-01	2.047E-01	1.997E-01
f13	4.443E-01	3.567E-01	3.695E-01	3.667E-01	3.384E-01	**3.296E-01**	3.536E-01	3.604E-01	3.701E-01	3.515E-01	3.836E-01
f14	2.593E-01	2.273E-01	2.133E-01	**2.122E-01**	2.275E-01	2.239E-01	2.197E-01	2.265E-01	2.343E-01	2.184E-01	2.371E-01
f15	2.192E+01	1.640E+01	1.506E+01	**1.296E+01**	1.553E+01	1.550E+01	1.416E+01	1.324E+01	1.783E+01	1.494E+01	1.514E+01
f16	1.060E+01	1.067E+01	1.053E+01	1.050E+01	1.050E+01	1.062E+01	1.034E+01	1.059E+01	1.060E+01	1.030E+01	1.064E+01
f17	1.050E+05	1.170E+06	1.180E+05	1.540E+05	1.450E+05	1.840E+05	2.030E+05	2.340E+05	2.730E+05	3.710E+05	5.780E+05
f18	1.150E+07	8.560E+06	8.620E+05	6.870E+05	1.720E+05	7.930E+05	2.630E+06	6.060E+05	4.040E+05	7.959E+04	7.810E+06
f19	2.050E+01	1.985E+01	1.350E+01	1.524E+01	2.554E+01	1.477E+01	9.771E+00	1.966E+01	2.310E+01	2.263E+01	1.333E+01
f20	2.984E+04	2.415E+04	2.357E+04	2.240E+04	1.927E+04	2.481E+04	2.092E+04	2.320E+04	2.310E+04	1.876E+04	2.254E+04
f21	2.610E+05	5.550E+05	1.670E+05	2.100E+05	2.870E+05	2.450E+05	2.280E+05	3.170E+05	3.730E+05	3.800E+05	3.920E+05
f22	6.217E+02	4.973E+02	5.113E+02	5.585E+02	5.473E+02	5.175E+02	5.325E+02	5.232E+02	5.259E+02	**4.769E+02**	5.100E+02
f23	3.181E+02	3.161E+02	3.164E+02	3.164E+02	3.164E+02	3.166E+02	3.165E+02	3.168E+02	3.161E+02	3.167E+02	3.162E+02
f24	2.310E+02	2.292E+02	2.294E+02	2.294E+02	2.297E+02	2.291E+02	2.298E+02	2.294E+02	2.287E+02	2.288E+02	2.282E+02
f25	2.151E+02	2.143E+02	2.144E+02	2.159E+02	2.145E+02	2.144E+02	2.143E+02	2.148E+02	2.144E+02	2.144E+02	2.152E+02
f26	1.204E+02	1.204E+02	1.237E+02	1.171E+02	1.137E+02	1.170E+02	1.170E+02	1.270E+02	1.071E+02	1.270E+02	1.137E+02
f27	5.985E+02	5.476E+02	5.567E+02	5.467E+02	5.810E+02	5.934E+02	5.531E+02	5.705E+02	5.994E+02	5.819E+02	5.571E+02
f28	1.574E+03	1.610E+03	1.815E+03	1.601E+03	1.511E+03	1.839E+03	1.514E+03	1.821E+03	1.524E+03	1.723E+03	**1.504E+03**
f29	2.477E+03	1.189E+03	9.830E+02	9.545E+02	1.074E+03	1.009E+03	1.013E+03	1.402E+03	1.080E+03	1.290E+03	2.990E+03
f30	5.438E+03	3.848E+03	3.006E+03	2.886E+03	2.809E+03	3.481E+03	3.172E+03	3.546E+03	3.342E+03	3.428E+03	3.591E+03

Figure 6. Result of the ASSKFR_a^{fit} experiment (Δ= {55%, 60%, 65%, 70%, 75%, 80%, 85%, 90%, 95%}).

Table 2. Statistical analysis of the ASSKFR_a^{fit} experiment.

	S-SKF vs $\mathbf{ASSKFR}_a^{fit}$			A-SKF vs $\mathbf{ASSKFR}_a^{fit}$	
Δ	*R+*	*R−*	Δ	*R+*	*R−*
5%	42	423	5%	57	408
10%	33	432	10%	83	382
15%	50	415	15%	66	399
20%	44	421	20%	56	409
25%	40	425	25%	86	379
30%	28	437	30%	53	412
35%	59	406	35%	68	397
40%	61	404	40%	97	368
45%	43	422	45%	111	324
50%	83.5	381.5	50%	156	309
55%	90	375	55%	197	268
60%	72	393	60%	137	328
65%	94	371	65%	192	273
70%	75	390	70%	182	283
75%	47	418	75%	146	289
80%	139	326	80%	207	258
85%	138	327	85%	174	291
90%	140	325	90%	211	254
95%	147	318	95%	152	313

On the other hand, based on from the ASSKFR_s^{fit} experiment, the average fitness error values are shown in Figure 7 and Figure 8. It is observed that a greater number of the best average fitness error was found by ASSKFR_s^{fit} with Δ = {5%}. The results of Wilcoxon signed rank test [37] are shown in Table 3. ASSKFR_s^{fit} outperformed SSKF with significance level ranging from 10% to 1%. The statistically better performance is observed for all value of Δ. The ASSKFR_s^{fit} with Δ = {5%, 10%, 15%, 25%} are significantly better than ASKF with significance level of 1% for Δ = {5%, 10%} and significance level of 10% for Δ = {15%, 25%}.

Conclusions

The SKF algorithm can be implemented by two different iteration strategies, either synchronous or asynchronous. A variant of SKF algorithm termed as ASSKFR that applied switching between synchronous and asynchronous is studied in this paper. The promising result showed the strength of the ASSKFR.

mekatronika – Journal of Intelligent Manufacturing & Mechatronics
VOL. 01, ISSUE 02, 45 – 65
DOI: https://doi.org/10.15282/mekatronika.v1i2.4241

Function ID	S-SKF	A-SKF	Δ									
			5%	10%	15%	20%	25%	30%	35%	40%	45%	50%
f1	4.860E+05	1.100E+07	3.220E+05	5.320E+05	3.760E+05	3.540E+05	5.110E+05	4.250E+05	4.060E+05	6.490E+05	5.210E+05	3.870E+05
f2	2.450E+08	1.290E+06	3.803E+04	**2.995E+04**	5.140E+06	1.460E+06	6.360E+05	4.850E+06	1.590E+07	4.520E+06	1.340E+07	1.260E+07
f3	1.841E+04	9.901E+03	**4.222E+03**	8.604E+03	9.132E+03	1.000E+04	1.192E+04	1.205E+04	1.388E+04	1.378E+04	1.592E+04	1.059E+04
f4	3.646E+01	1.177E+02	1.901E+01	**9.802E+00**	2.132E+01	2.216E+01	2.873E+01	3.659E+01	1.177E+01	2.749E+01	1.337E+01	2.922E+01
f5	2.002E+01	2.001E+01	**2.000E+01**	**2.000E+01**	2.000E+01	2.000E+01	2.000E+01	**2.000E+01**	2.000E+01	2.000E+01	2.000E+01	2.001E+01
f6	2.195E+01	1.817E+01	1.764E+01	1.788E+01	1.764E+01	1.889E+01	**1.739E+01**	1.878E+01	1.984E+01	1.832E+01	1.889E+01	1.845E+01
f7	1.635E-01	**8.444E-02**	1.240E-01	1.129E-01	1.369E-01	1.312E-01	1.835E-01	2.432E-01	1.227E-01	2.715E-01	9.788E-02	2.957E-01
f8	5.878E+00	5.473E+00	**4.803E-01**	1.070E+00	1.372E+00	1.928E+00	2.389E+00	2.496E+00	2.790E+00	2.699E+00	2.907E+00	2.940E+00
f9	9.087E+01	**7.526E+01**	8.482E+01	8.932E+01	8.733E+01	9.847E+01	8.161E+01	8.790E+01	9.201E+01	8.759E+01	8.913E+01	9.228E+01
f10	2.263E+02	1.620E+02	3.652E+01	**2.938E+01**	8.092E+01	1.188E+02	1.089E+02	1.203E+02	1.540E+02	1.515E+02	1.420E+02	1.496E+02
f11	2.640E+03	2.585E+03	2.818E+03	2.745E+03	2.769E+03	2.827E+03	2.668E+03	**2.585E+03**	2.730E+03	2.737E+03	2.758E+03	2.649E+03
f12	3.592E-01	2.099E-01	**1.979E-01**	2.292E-01	2.680E-01	2.442E-01	2.847E-01	2.769E-01	3.093E-01	2.660E-01	2.823E-01	3.005E-01
f13	4.443E-01	**3.567E-01**	4.398E-01	4.339E-01	4.162E-01	4.191E-01	4.423E-01	4.390E-01	4.279E-01	4.414E-01	4.511E-01	4.159E-01
f14	2.593E-01	**2.273E-01**	2.462E-01	2.700E-01	2.479E-01	2.694E-01	2.622E-01	2.541E-01	2.674E-01	2.636E-01	2.736E-01	2.648E-01
f15	2.192E+01	**1.640E+01**	1.884E+01	2.247E+01	2.071E+01	2.037E+01	2.457E+01	2.126E+01	2.318E+01	2.397E+01	2.376E+01	1.728E+01
f16	1.060E+01	1.067E+01	**1.025E+01**	1.080E+01	1.054E+01	1.055E+01	1.050E+01	1.074E+01	1.039E+01	1.065E+01	1.059E+01	1.077E+01
f17	1.050E+05	1.170E+06	1.270E+05	1.440E+05	1.890E+05	1.290E+05	1.630E+05	1.180E+05	1.730E+05	1.310E+05	1.450E+05	1.430E+05
f18	1.150E+07	8.560E+06	**1.914E+03**	1.958E+03	2.560E+03	2.674E+03	2.629E+03	3.197E+03	5.923E+04	1.913E+04	1.600E+05	1.290E+05
f19	2.050E+01	1.985E+01	**7.894E+00**	1.395E+01	1.038E+01	1.459E+01	1.699E+01	2.387E+01	1.543E+01	1.757E+01	1.748E+01	1.832E+01
f20	2.984E+04	2.415E+04	**4.906E+03**	1.007E+04	1.267E+04	1.479E+04	1.429E+04	1.543E+04	2.056E+04	1.943E+04	1.972E+04	2.190E+04
f21	2.610E+05	5.550E+05	**1.270E+05**	2.880E+05	2.550E+05	2.040E+05	2.130E+05	2.020E+05	2.280E+05	2.150E+05	2.750E+05	2.090E+05
f22	6.217E+02	**4.973E+02**	5.370E+02	5.384E+02	5.353E+02	5.648E+02	5.381E+02	5.976E+02	6.209E+02	6.075E+02	5.736E+02	6.261E+02
f23	3.181E+02	3.161E+02	**3.158E+02**	3.161E+02	3.165E+02	3.163E+02	3.161E+02	3.165E+02	3.164E+02	3.168E+02	3.166E+02	3.167E+02
f24	2.310E+02	**2.292E+02**	2.304E+02	**2.292E+02**	2.323E+02	2.304E+02	2.316E+02	2.320E+02	2.303E+02	2.323E+02	2.319E+02	2.313E+02
f25	2.151E+02	2.143E+02	**2.128E+02**	2.129E+02	2.140E+02	2.145E+02	2.150E+02	2.146E+02	2.164E+02	2.140E+02	2.129E+02	2.140E+02
f26	1.204E+02	1.204E+02	**1.005E+02**	1.038E+02	1.104E+02	1.138E+02	1.071E+02	1.105E+02	1.038E+02	1.105E+02	1.038E+02	1.337E+02
f27	5.985E+02	**5.476E+02**	6.432E+02	6.788E+02	6.444E+02	6.482E+02	7.190E+02	6.310E+02	6.089E+02	6.611E+02	7.083E+02	6.697E+02
f28	1.574E+03	1.610E+03	1.538E+03	1.515E+03	1.560E+03	1.507E+03	**1.356E+03**	1.521E+03	1.649E+03	1.670E+03	1.485E+03	1.721E+03
f29	2.477E+03	1.189E+03	1.085E+03	1.115E+03	1.172E+03	1.114E+03	1.107E+03	1.102E+03	1.128E+03	1.122E+03	1.509E+03	1.108E+03
f30	5.438E+03	3.848E+03	3.326E+03	3.464E+03	**3.110E+03**	3.362E+03	3.690E+03	3.879E+03	4.128E+03	3.862E+03	3.646E+03	3.709E+03

Figure 7. Result of the ASSKFR$_s^{fit}$ experiment (Δ= {5%, 10%, 15%, 20%, 25%, 30%, 35%, 40%, 45%, 50%}).

References

[1] Ibrahim, Z., Abdul Aziz, N.H., Ab. Aziz, N.A., Razali, R., and Mohamad, M.S. (2016). Simulated Kalman filter: a novel estimation-based metaheuristic optimization algorithm. Advanced Science Letters, vol. 22, pp. 2941-2946.

[2] Abd Aziz, N.H., Ibrahim, Z., Razali, S., and Ab. Aziz, N.A. (2016) Estimation-based metaheuristics: a new branch of computational intelligence. The National Conference for Postgraduate Research, pp. 469-476.

[3] Ibrahim, Z., Abdul Aziz, N.H., Ab Aziz, N.A., Razali, S., Shapiai, M.I., Nawawi, S.W., and Mohamad, M.S. (2015) A Kalman filter approach for solving unimodal optimization problems. ICIC Express Letters, vol. 9, pp. 3415-3422.

[4] Kalman, R.E. (1960) A new approach to linear filtering and prediction problems. ASME Journal of Basic Engineering, vol. 82, pp. 35-45.

[5] Abd Aziz, N.H., Ibrahim, Z., Razali, S., Bakare, T.A., and Ab. Aziz, N.A. (2016). How important the error covariance in simulated Kalman filter?. The National Conference for Postgraduate Research, pp. 315-320.

[6] Abd Aziz, N.H., Ab. Aziz, N.A., Mat Jusof, M.F., Razali, S., Ibrahim, Z., Adam, A., and Shapiai, M.I. (2018). An analysis on the number of agents towards the performance of the simulated Kalman filter optimizer. 8th International Conference on Intelligent Systems, Modelling and Simulation, pp. 16-21.

[7] Md Yusof, Z., Ibrahim, I., Satiman, S.N., Ibrahim, Z., Abd Aziz, N.H., and Ab. Aziz, N.A. (2015). BSKF: binary simulated Kalman filter. Third International Conference on Artificial Intelligence, Modelling and Simulation, pp. 77-81.

[8] Md Yusof, Z., Ibrahim, I., Ibrahim, Z., Abas, K.H., Ab. Aziz, N.A., Abd Aziz, N.H., and Mohamad, M.S. (2016). Local optimum distance evaluated simulated Kalman filter for combinatorial optimization problems. The National Conference for Postgraduate Research, pp. 892-901.

[9] Md Yusof, Z., Ibrahim, I., Ibrahim, Z., Mohd Azmi, K.Z., Ab. Aziz, N.A., Abd Aziz, N.H., and Mohamad, M.S. (2016). Distance evaluated simulated Kalman filter for combinatorial optimization problems. ARPN Journal of Engineering and Applied Sciences, vol. 11, pp. 4904-4910.

[10] Md Yusof, Z., Ibrahim, I., Ibrahim, Z., Mohd Azmi, K.Z., Ab. Aziz, N.A., Abd Aziz, N.H., and Mohamad, M.S. (2016). Angle modulated simulated Kalman filter algorithm for combinatorial optimization problems. ARPN Journal of Engineering and Applied Sciences, vol. 11, pp. 4854-4859.

*CORRESPONDING AUTHOR | Nor Azlina Ab. Aziz | ✉ azlina.aziz@mmu.edu.my

mekatronika – Journal of Intelligent Manufacturing & Mechatronics
VOL. 01, ISSUE 02, 45 – 65
DOI: https://doi.org/10.15282/mekatronika.v1i2.4241

Function ID	S-SKF	A-SKF	Δ								
			55%	60%	65%	70%	75%	80%	85%	90%	95%
f1	4.860E+05	1.100E+07	4.280E+05	4.300E+05	4.350E+05	4.050E+05	3.070E+05	2.960E+05	3.340E+05	3.140E+05	**2.750E+05**
f2	2.450E+08	1.290E+06	6.820E+06	1.660E+06	7.260E+06	2.050E+06	5.470E+06	3.580E+07	1.760E+07	2.270E+07	2.170E+07
f3	1.841E+04	9.901E+03	1.340E+04	1.350E+04	1.473E+04	1.519E+04	1.308E+04	1.274E+04	1.429E+04	1.234E+04	1.479E+04
f4	3.646E+01	1.177E+02	1.964E+01	3.386E+01	2.324E+01	2.816E+01	1.748E+01	4.365E+01	4.030E+01	1.561E+01	2.824E+01
f5	2.002E+01	2.001E+01	2.000E+01	2.000E+01	2.000E+01	2.000E+01	2.000E+01	2.000E+01	2.000E+01	2.000E+01	2.001E+01
f6	2.195E+01	1.817E+01	1.845E+01	1.896E+01	1.791E+01	1.853E+01	1.802E+01	1.903E+01	1.864E+01	1.816E+01	1.898E+01
f7	1.635E-01	**8.444E-02**	1.344E-01	1.760E-01	1.554E-01	1.555E-01	1.624E-01	4.045E-01	2.018E-01	2.991E-01	2.080E-01
f8	5.878E+00	5.473E+00	3.751E+00	3.730E+00	2.863E+00	2.564E+00	3.749E+00	2.659E+00	3.369E+00	4.205E+00	4.763E+00
f9	9.087E+01	**7.526E+01**	8.579E+01	8.592E+01	8.268E+01	8.129E+01	8.504E+01	8.945E+01	8.582E+01	8.814E+01	8.692E+01
f10	2.263E+02	1.620E+02	1.109E+02	1.065E+02	1.122E+02	1.294E+02	1.195E+02	1.269E+02	1.360E+02	1.672E+02	1.454E+02
f11	2.640E+03	2.585E+03	2.677E+03	2.676E+03	2.801E+03	2.783E+03	2.676E+03	2.816E+03	2.852E+03	2.758E+03	2.709E+03
f12	3.592E-01	2.099E-01	2.930E-01	2.792E-01	2.677E-01	3.069E-01	3.162E-01	2.694E-01	2.535E-01	2.940E-01	3.396E-01
f13	4.443E-01	**3.567E-01**	4.725E-01	4.340E-01	4.082E-01	4.394E-01	4.166E-01	4.570E-01	4.788E-01	4.452E-01	4.252E-01
f14	2.593E-01	**2.273E-01**	2.629E-01	2.813E-01	2.759E-01	2.683E-01	2.861E-01	2.757E-01	2.786E-01	2.811E-01	2.807E-01
f15	2.192E+01	**1.640E+01**	2.148E+01	2.328E+01	2.517E+01	1.945E+01	2.339E+01	2.658E+01	2.039E+01	2.354E+01	2.379E+01
f16	1.060E+01	1.067E+01	1.062E+01	1.092E+01	1.071E+01	1.069E+01	1.041E+01	1.078E+01	1.044E+01	1.072E+01	1.058E+01
f17	1.050E+05	1.170E+06	1.850E+05	9.815E+04	1.700E+05	1.200E+05	1.050E+05	1.140E+05	1.110E+05	1.440E+05	**8.112E+04**
f18	1.150E+07	8.560E+06	9.437E+03	1.848E+04	1.167E+04	5.750E+05	4.992E+03	1.590E+05	4.685E+04	2.060E+05	4.970E+05
f19	2.050E+01	1.985E+01	1.949E+01	1.504E+01	1.711E+01	2.809E+01	1.948E+01	2.794E+01	2.034E+01	1.668E+01	1.241E+01
f20	2.984E+04	2.415E+04	2.455E+04	1.993E+04	2.073E+04	1.868E+04	2.153E+04	2.396E+04	2.317E+04	2.390E+04	1.825E+04
f21	2.610E+05	5.550E+05	2.860E+05	1.650E+05	2.160E+05	2.040E+05	2.260E+05	2.220E+05	2.160E+05	2.150E+05	1.850E+05
f22	6.217E+02	**4.973E+02**	5.921E+02	6.431E+02	5.961E+02	6.152E+02	6.099E+02	6.376E+02	7.206E+02	5.924E+02	5.893E+02
f23	3.181E+02	3.161E+02	3.171E+02	3.165E+02	3.165E+02	3.166E+02	3.163E+02	3.163E+02	3.167E+02	3.172E+02	3.167E+02
f24	2.310E+02	**2.292E+02**	2.315E+02	2.312E+02	2.305E+02	2.319E+02	2.319E+02	2.324E+02	2.296E+02	2.340E+02	2.308E+02
f25	2.151E+02	2.143E+02	2.140E+02	2.134E+02	2.142E+02	2.145E+02	2.152E+02	2.129E+02	2.147E+02	2.149E+02	2.150E+02
f26	1.204E+02	1.204E+02	1.171E+02	1.104E+02	1.171E+02	1.104E+02	1.105E+02	1.138E+02	1.038E+02	1.071E+02	1.171E+02
f27	5.985E+02	**5.476E+02**	6.467E+02	6.676E+02	6.648E+02	6.649E+02	6.720E+02	5.641E+02	7.228E+02	6.624E+02	7.000E+02
f28	1.574E+03	1.610E+03	1.569E+03	1.642E+03	1.435E+03	1.466E+03	1.495E+03	1.475E+03	1.501E+03	1.441E+03	1.770E+03
f29	2.477E+03	1.189E+03	1.716E+03	1.200E+03	1.215E+03	**1.069E+03**	1.369E+03	1.213E+03	1.194E+03	1.820E+03	1.241E+03
f30	5.438E+03	3.848E+03	3.712E+03	3.972E+03	4.832E+03	4.607E+03	4.615E+03	4.139E+03	6.576E+03	4.577E+03	4.239E+03

Figure 8. Result of the ASSKFR$_s^{fit}$ experiment (Δ= {55%, 60%, 65%, 70%, 75%, 80%, 85%, 90%, 95%}).

Table 3. Statistical analysis of the ASSKFR$_s^{fit}$ experiment.

S-SKF vs **ASSKFR**$_s^{fit}$			A-SKF vs **ASSKFR**$_s^{fit}$		
Δ	$R+$	$R-$	Δ	$R+$	$R-$
5%	63	402	5%	101	364
10%	134	331	10%	102	333
15%	74	391	15%	147	318
20%	80	385	20%	182	283
25%	115	350	25%	143	322
30%	84	381	30%	210	255
35%	115	350	35%	233	232
40%	144	321	40%	228	237
45%	143	322	45%	205	260
50%	144	321	50%	224	241
55%	108	357	55%	232	233
60%	101	364	60%	243	222
65%	87	378	65%	221	244
70%	96	369	70%	226	239
75%	64	371	75%	225	240
80%	130	335	80%	244	221
85%	130	335	85%	243	222
90%	101	364	90%	255	210
95%	80	385	95%	257	208

*CORRESPONDING AUTHOR | Nor Azlina Ab. Aziz | ✉ azlina.aziz@mmu.edu.my

[11] Muhammad, B., Ibrahim, Z., Mat Jusof, M.F., Ab. Aziz, N.A., Abd Aziz, N.H., and Mokhtar, N. (2017). A hybrid simulated Kalman filter - gravitational search algorithm (SKF-GSA). International Conference on Artificial Life and Robotics, pp. 707–710.

[12] Muhammad, B., Ibrahim, I., Mohd Azmi, K.Z., Abas, K.H., Ab. Aziz, N.A., Abd Aziz, N.H., and Mohamad, M.S. (2016). Performance evaluation of hybrid SKF algorithms: hybrid SKF-PSO and hybrid SKF-GSA. The National Conference for Postgraduate Research, pp. 865-874.

[13] Muhammad, B., Ibrahim, Z., Mohd Azmi, K.Z., Abas, K.H., Ab. Aziz, N.A., Abd Aziz, N.H., and Mohamad, M.S. (2016). Four different methods to hybrid simulated Kalman filter (SKF) with particle swarm optimization (PSO), The National Conference for Postgraduate Research, pp. 843-853.

[14] Muhammad, B., Ibrahim, Z., Mohd Azmi, K.Z., Abas, K.H., Ab. Aziz, N.A., Abd Aziz, N.H., and Mohamad, M.S. (2016). Four different methods to hybrid simulated Kalman filter (SKF) with gravitational search algorithm (GSA). The National Conference for Postgraduate Research, pp. 854-864.

[15] Muhammad, B., Ibrahim, Z., Ghazali, K.H., Mohd Azmi, K.Z., Ab. Aziz, N.A., Abd Aziz, N.H., and Mohamad, M.S. (2015). A new hybrid simulated Kalman filter and particle swarm optimization for continuous numerical optimization problems. ARPN Journal of Engineering and Applied Sciences, vol. 10, pp. 17171-17176.

[16] Ibrahim, Z., Mohd Azmi, K.Z., Ab. Aziz, N.A., Abd Aziz, N.H., Muhammad, B., Mat Jusof, M.F., and Shapiai, M.I. (2018). An oppositional learning prediction operator for simulated Kalman filter. The 3rd International Conference on Computational Intelligence and Applications, pp. 139-143.

[17] Mohd Azmi, K.Z., Ibrahim, Z., Pebrianti, D., Mat Jusof, M.F., Abdul Aziz, N.H., Ab. Aziz, N.A. (2019). Enhancing simulated Kalman filter algorithm using current optimum opposition-based learning. Mekatronika, vol. 1, pp. 1-13.

[18] Abd Aziz, N.H., Ibrahim, Z., Ab. Aziz, N.A., and Razali, S. (2017). Parameter-less simulated Kalman filter. International Journal of Software Engineering and Computer Systems, vol. 3, pp. 129-137.

[19] Abd Aziz, N.H., Ab. Aziz, N.A., Ibrahim, Z., Razali, S., Mat Jusof, M.F., Abas, K.H., Mohamad, M.S., and Mokhtar, N. (2017). Simulated Kalman filter with randomized Q and R parameters. International Conference on Artificial Life and Robotics, pp. 711-714.

[20] Lazarus, K., Noordin, N.H., Mat Jusof, M.F., Ibrahim, Z., and Abas, K.H. (2017). Adaptive beamforming algorithm based on a simulated Kalman filter. International Journal of Simulation: Systems, Science and Technology, vol. 18, pp. 10.1-10.5.

[21] Lazarus, K., Noordin, N.H., Mohd Azmi, K.Z., Abd Aziz, K.Z., and Ibrahim, Z. (2016). Adaptive beamforming algorithm based on generalized opposition-based simulated Kalman filter. The National Conference for Postgraduate Research, pp. 1-9.

[22] Lazarus, K., Noordin, N.H., Ibrahim, Z., Mat Jusof, M.F., Mohd Faudzi, M.A., Subari, N., and Mohd Azmi, K.Z. (2017). An opposition-based simulated Kalman filter algorithm for adaptive beamforming. IEEE International Conference on Applied System Innovation, pp. 91-94.

[23] Lazarus, K., Noordin, N.H., Ibrahim, Z., and Abas, K.H. (2016). Adaptive beamforming algorithm based on simulated Kalman filter. Asia Multi Conference on Modelling and Simulation, pp. 19-23.

[24] Md Yusof, Z., Satiman, S.N., Mohd Azmi, K.Z., Muhammad, B., Razali, S., Ibrahim, Z., Aspar, Z., and Ismail, S. (2015). Solving airport gate allocation problem using simulated Kalman filter. International Conference on Knowledge Transfer, pp. 121-127.

[25] Mohd Azmi, K.Z., Md Yusof, Z., Satiman, S.N., Muhammad, B., Razali, S., Ibrahim, Z., Ab. Aziz, N.A., and Abd Aziz, N.H. (2016). Solving airport gate allocation problem using angle modulated simulated Kalman filter. The National Conference for Postgraduate Research, pp. 875-885.

[26] Muhammad, B., Mat Jusof, M.F., Shapiai, M.I., Adam, A., Md Yusof, Z., Mohd Azmi, K.Z., Abdul Aziz, N.H., Ibrahim, Z., and Mokhtar, N. (2018). Feature selection using binary simulated Kalman filter for peak classification of EEG signals. 2018 8th International Conference on Intelligent Systems, Modelling and Simulation, pp. 1-6.

[27] Adam, A., Ibrahim, Z., Mokhtar, N., Shapiai, M.I., Mubin, M., and Saad, I. (2016). Feature selection using angle modulated simulated Kalman filter for peak classification of EEG signals. SpringerPlus, vol. 5, 1580.

[28] Muhammad, B., Mohd Azmi, K.Z., Ibrahim, Z., Mohd Faudzi, A.A., and Pebrianti, D. (2018). Simultaneous computation of model order and parameter estimation for system identification based on opposition-based simulated Kalman filter. SICE International Symposium on Control Systems 2018, pp. 105-112.

[29] Mohd Azmi, K.Z., Ibrahim, Z., Pebrianti, D., and Mohamad, M.S. (2017). Simultaneous computation of model order and parameter estimation for ARX model based on single and multi swarm simulated Kalman filter. Journal of Telecommunication, Electronic, and Computer Engineering, vol. 9, pp. 151-155.

[30] Ann, N.Q., Pebrianti, D., Bayuaji, L., Daud, M.R., Samad, R., Ibrahim, Z., Hamid, R., and Syafrullah, M. (2018). SKF-based image template matching for distance measurement by using stereo vision. Intelligent Manufacturing and Mechatronics, pp. 439-447.

[31] Ann, N.Q., Pebrianti, D., Ibrahim, Z., Mat Jusof, M.F., Bayuaji, L., and Abdullah, N.R.H. (2018). Illumination-invariant image matching based on simulated Kalman filter (SKF). Journal of Telecommunication, Electronics and Computer Engineering, vol. 10, pp. 31-36.

[32] Muhammad, B., Pebrianti, D., Abdul Ghani, N., Abd Aziz, N.H., Ab. Aziz, N.A., Mohamad, M.S., Shapiai, M.I., and Ibrahim, Z. (2018). An application of simulated Kalman filter optimization algorithm for parameter tuning in proportional-integral-derivative controllers for automatic voltage regulator system. SICE International Symposium on Control Systems 2018, pp. 113-120.

[33] Abd Aziz, N.H., Ab. Aziz, N.A, Ibrahim, Z., Razali, S., Abas, K.H., and Mohamad, M.S. (2016). A Kalman filter approach to PCB drill path optimization problem. IEEE Conference on Systems, Process and Control, pp. 33-36.

[34] Abd Aziz, N.H., Ibrahim, Z., Ab. Aziz, N.A., Md Yusof, Z., and Mohamad, M.S. (2018). Single-solution simulated Kalman filter algorithm for routing in printed circuit board drilling process. Intelligent Manufacturing and Mechatronics, pp. 649-655.

[35] Ab Aziz, N.A., Ibrahim, Z., Abdul Aziz, N.H., and Ab Rahman, T. (2018). Asynchronous simulated Kalman filter optimization algorithm. International Journal of Engineering and Technology(UAE), vol. 7, pp. 44-49.

[36] Liang, J.J., Qu, B.Y., Suganthan, P.N. (2013). Problem definitions and evaluation criteria for the CEC 2014 special session and competition on single objective real-parameter numerical optimization. Tech. Rep. 201311. Computational Intelligence Laboratory, Zhengzhou University, Zhengzhou, China and Nanyang Technological University, Singapore.

[37] García, S., Molina, D., Lozano, M., Herrera, F. (2008). A study on the use of non-parametric tests for analyzing the evolutionary algorithms' behaviour: a case study on the CEC'2005 special session on real parameter optimization. Journal of Heuristics, vol. 15, pp. 617-644.